CWP-168
May 1995

Test on Marmousi Data of velocity analysis by perturbation

Zhenyue Liu

Excerpt from

— Doctoral Thesis —

Mathematical and Computer Sciences

Partially supported by the Office of Naval Research,
Contract Number N00014-94-1-0530.

Center for Wave Phenomena
Colorado School of Mines
Golden, Colorado 80401
303/273-3557

DEPARTMENT OF THE NAVY
OFFICE OF NAVAL RESEARCH
SEATTLE REGIONAL OFFICE
1107 NE 45TH STREET, SUITE 350
SEATTLE WA 98105-4631

IN REPLY REFER TO:

4330
ONR 247
11 Jul 97

From: Director, Office of Naval Research, Seattle Regional Office, 1107 NE 45th St., Suite 350, Seattle, WA 98105
To: Defense Technical Center, Attn: P. Mawby, 8725 John J. Kingman Rd., Suite 0944, Ft. Belvoir, VA 22060-6218

Subj: RETURNED GRANTEE/CONTRACTOR TECHNICAL REPORTS

1. This confirms our conversations of 27 Feb 97 and 11 Jul 97. Enclosed are a number of technical reports which were returned to our agency for lack of clear distribution availability statement. This confirms that all reports are unclassified and are "APPROVED FOR PUBLIC RELEASE" with no restrictions.

2. Please contact me if you require additional information. My e-mail is *silverr@onr.navy.mil* and my phone is (206) 625-3196.

ROBERT J. SILVERMAN

Test on Marmousi data of velocity analysis by perturbation

Zhenyue Liu and Norman Bleistein

ABSTRACT

Velocity model determination on the Marmousi data is a major challenge for current velocity analysis methods because of the extreme complexity of the model. A new velocity analysis method has been developed and is tested on the Marmousi data. This method characterizes a velocity distribution by the macro model and uses an analytical formula to update velocity. Our formula estimates the update in velocity by computing a derivative function of imaged depths with respect to velocity in a general background medium context. This formula is more accurate than conventional ones based on hyperbolic residual moveout when the medium has strongly lateral velocity variations. The test results show our velocity analysis method to be superior for complex media such as in the Marmousi model.

INTRODUCTION

The Marmousi model is a 2D model with considerable complexity of structures and a realistic distribution of reflectors. Prestack data from it provide a stiff challenge to methods for estimating velocities from seismic data.

Strong velocity variations in the Marmousi model suggest that the method for velocity estimation should not be based on the assumption of hyperbolic residual moveout. Liu and Bleistein (1994) proposed an approach to migration velocity analysis that characterizes a velocity distribution by using the macro model—consisting of velocities and velocity interfaces. The model is determined by layer-stripping, in a top-down procedure; the velocity of each layer (assumed constant or constant gradient) is updated iteratively by using an analytical formula; and the velocity interface is imaged by using the corrected velocity. In order to handle nonhyperbolic residual moveout, the velocity estimation in the proposed formula is implemented by computing a derivative function of imaged depths with respect to velocity in a general context of the background medium. This derivative function can be calculated by using the ratio of two migration outputs. This ratio yields the stationary value of the expression for the derivative function—exactly the result we need. This is the same

method as is used in Bleistein, et al., (1987) to compute the cosine of the incident angle at a reflector.

The efficiency of a velocity analysis approach surely depends on the choice of migration algorithm used. In general, integral-type migration approaches, such as Kirchhoff or Gaussian beam, are preferable, because those methods can be implemented either in common-shot gathers or in common-offset gathers, and have the flexibility to image the targeted structures in which velocity is being estimated. Besides efficiency, accuracy should be considered as well. For imaging complex structures, a migration algorithm should be designed to handle turning waves and caustic regions.

In the Kirchhoff integral, traveltime calculation by ray tracing or finite differencing dominates the total cost. Finite differencing calculates only the first-arrival traveltime, so this approach works fast but fails in calculation of major-energy traveltimes in caustic regions (Geoltrain and Brac, 1993). The paraxial ray method, in contrast, shows advantages in handling multivalued traveltimes and caustics. This method uses information from the standard dynamic ray-tracing method to extrapolate traveltimes and ray amplitudes at receivers in the vicinity of a central ray (Beydoun and Keho, 1987). However, the traveltime calculation by the paraxial ray tracer is generally more costly than that by finite differencing. Here, finite differencing is initially used in the migration implementation for velocity analysis in the area of the Marmousi model where the first arrivals carry the major energy. In the central bottom parts, a paraxial ray tracing algorithm is used to implement Kirchhoff migration. In this approach, the traveltime corresponding to the major energy is chosen when multiple arrivals exist.

METHODOLOGY

If an incorrect velocity is used in prestack migration, the imaged depths from different offsets in a common-image-gather(CIG) will differ from each other. A CIG is a gather in which migrated traces have the same lateral image location. In this situation, a residual moveout is observed in migrated data. The principle of velocity analysis is to correct the velocity so that the imaged depths at each common-image-gather are close to each other. For this purpose, one needs a quantitative relationship between the residual moveout and the velocity error. Here, we present a representation for residual moveout derived by using a perturbation method. This representation is valid for any offset, reflector dip and velocity distribution.

Perturbation formula for velocity estimation

We denote by $\boldsymbol{x}$ a 2-D vector, $\boldsymbol{x} = (x, z)$. Let x_s be the source position and x_r be the receiver position on the surface. For any point X below the surface, $\tau_s(x_s, \boldsymbol{x})$ or $\tau_r(\boldsymbol{x}, x_r)$, respectively, denote traveltimes from x_s to $\boldsymbol{x}$, or $\boldsymbol{x}$ to x_r.

Suppose we know the total reflection travetime function $t(y, h)$ (therefore, $\partial t/\partial y$) that depends on midpoint y and half-offset h. Given a velocity function $v(x, z)$, then,

for each h, the reflector is determined by

$$\tau_s(x_s, \boldsymbol{x}) + \tau_r(\boldsymbol{x}, x_r) = t(y, h), \tag{1}$$

$$\frac{\partial \tau_s}{\partial y} + \frac{\partial \tau_r}{\partial y} = \frac{\partial t}{\partial y}. \tag{2}$$

In a common image gather, the imaged depth z can be determined as a function of h. If the migration velocity equals the true velocity, then the imaged depth z will be independent of offset h; otherwise—for incorrect velocity—z varies with offset h. Consequently, the imaged depths in common image gathers (CIGs) provide information on velocity distribution.

Equations (1) and (2) are valid even if the migration velocity is wrong. The dependency of traveltime on velocity in equations (1) and (2) implies that this equation system displays a general relationship between the imaged depth and migration velocity. However, this equation system is nonlinear, making it difficult to solve directly for velocity. Here, we use a mathematical tool—perturbation—to linearize this equation system by considering for all perturbations in model parameters.

Suppose that the velocity distribution v is characterized by a parameter or a family of parameters, λ,

$$v = v(\boldsymbol{x}; \lambda).$$

For example, when $v(\boldsymbol{x}; \lambda) = v_0 + ax + bz$, λ is any set of one to three parameters chosen from v_0, a, and b. Thus, the problem of velocity estimation becomes a problem of parameter estimation. If there is a small perturbation $\delta\lambda = \lambda^* - \lambda$ between the true parameter and the parameter used in migration, then the imaged depth will have a corresponding perturbation

$$\delta z = g(x, h)\delta\lambda. \tag{3}$$

The derivative function g can be determined based on equations (1) and (2). To simplify the derivation, we suppose that λ is just a single parameter at first.

For a fixed image location x, we differentiate equation (1) with respect to λ. Note that y and z are functions of λ; then

$$\left[\frac{\partial \tau_s}{\partial y} + \frac{\partial \tau_r}{\partial y}\right]\frac{dy}{d\lambda} + \left[\frac{\partial \tau_s}{\partial \lambda} + \frac{\partial \tau_r}{\partial \lambda}\right] + \left[\frac{\partial \tau_s}{\partial z} + \frac{\partial \tau_r}{\partial z}\right]\frac{dz}{d\lambda} = \frac{\partial t}{\partial y}\frac{dy}{d\lambda}. \tag{4}$$

By using equation (2), the first term of the left side in equation (4) is balanced by the right-hand term. Therefore,

$$\left[\frac{\partial \tau_s}{\partial z} + \frac{\partial \tau_r}{\partial z}\right]\frac{dz}{d\lambda} = -\frac{\partial \tau_s}{\partial \lambda} - \frac{\partial \tau_r}{\partial \lambda}. \tag{5}$$

Let θ_s or θ_r be the angle between the raypath from the source or the receiver, and the vertical at $\boldsymbol{x}$; then

$$\frac{\partial \tau_s}{\partial z} = \frac{\cos\theta_s}{v(\boldsymbol{x}; \lambda)}, \qquad \frac{\partial \tau_r}{\partial z} = \frac{\cos\theta_r}{v(\boldsymbol{x}; \lambda)}, \tag{6}$$

By using the above equation, equation (5) is rewritten as

$$\frac{\cos\theta_s + \cos\theta_s}{v(\boldsymbol{x};\lambda)}\frac{dz}{d\lambda} = -\frac{\partial\tau_s}{\partial\lambda} - \frac{\partial\tau_r}{\partial\lambda}. \tag{7}$$

Thus the derivative of imaged depth with respect to λ is found by

$$g(x,h) = -\left[\frac{\partial\tau_s}{\partial\lambda} + \frac{\partial\tau_r}{\partial\lambda}\right]\frac{v(\boldsymbol{x};\lambda)}{\cos\theta_s + \cos\theta_r}. \tag{8}$$

The function g characterizes the relationship between the imaged depth and the migration velocity in a general medium context. The computation of this function will result in a new migration velocity analysis method, compared to conventional ones based on hyperbolic residual moveout.

The velocity estimation based on equation (3) has no limitation in velocity distribution and reflection geometry as long as the perturbation is small. When the velocity distribution is characterized by multiple parameters, $\hat{\lambda} = (\lambda_1, \lambda_2, ..., \lambda_n)^T$, the imaged-depth perturbation will depend on the perturbations of all these parameters. Therefore, equation (3) will be modified to

$$\delta z(x,h) = \sum_{i=1}^{n}\frac{\partial z}{\partial\lambda_i}\delta\lambda_i = \sum_{i=1}^{n} g_i(x,h)\delta\lambda_i, \tag{9}$$

where each derivative function is calculated by

$$g_i(x,h) = -\left[\frac{\partial\tau_s}{\partial\lambda_i} + \frac{\partial\tau_r}{\partial\lambda_i}\right]\frac{v(\boldsymbol{x};\hat{\lambda})}{\cos\theta_s + \cos\theta_r}. \tag{10}$$

Calculation of the function g

The function $g(y,h)$, which involves the derivatives of traveltimes with respect to the parameter λ, can be calculated by

$$\frac{\partial\tau}{\partial\lambda} = \int_L \frac{\partial}{\partial\lambda}\left(\frac{1}{v(\boldsymbol{x};\lambda)}\right)dL, \tag{11}$$

where L is the raypath from the source (or receiver) to the image point $\boldsymbol{x}$.

For each source or receiver, $\partial\tau/\partial\lambda$ can be determined from equation (11). Therefore, given an image point $\boldsymbol{x}$ and a specular source-receiver pair x_s and x_r, one can calculate g from formula (8). However, there is no explicit formula to represent the specular source-receiver pair from the image point for a complex medium. To solve this problem, we use the Kirchhoff integral to calculate g. In the Kirchhoff summation, we calculate two migration outputs which have the same phase but different amplitudes. One uses the original amplitude; the other one uses the original amplitude multiplied by the quantity g. Thus, the ratio of the amplitudes of these two outputs will evaluate g at the specular source-receiver position without requiring knowledge of the specular source-receiver pair. This technique, based on stationary-phase analysis, is the same as was used to determine the angle of reflection in Kirchhoff inversion (Bleistein et al., 1987).

Characterization of velocity distribution

Although equation (9) holds for any velocity distribution, the solution will be underdetermined and unstable if too many unknown parameters are involved. Consequently, it is essential to characterize the velocity distribution by choosing only a few appropriate parameters. Conventionally, one assumes that a velocity model consists of the construction of the macro-model (constant velocities and velocity interfaces). The interfaces divide the whole model into a number of blocks or layers (shown in Figure 1).

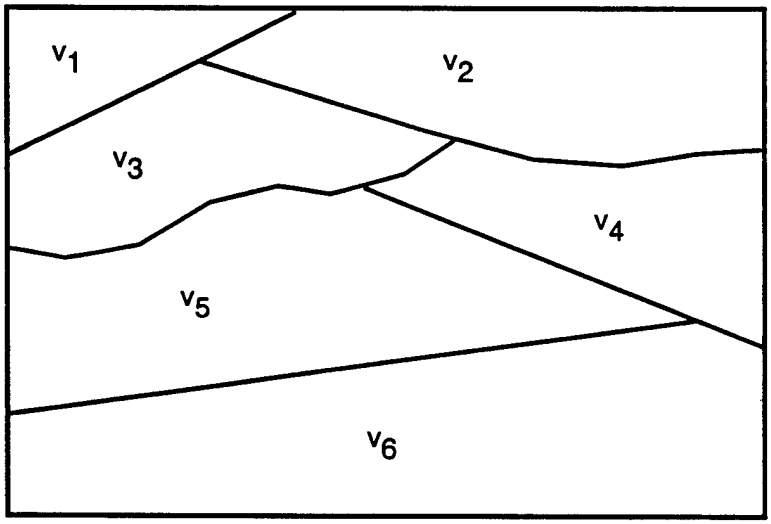

FIG. 1. Macro model.

Here, we replace constant velocity in each block by a linear function that is characterized by three parameters:

$$\lambda_1 + \lambda_2(z - z_0) + \lambda_3(x - x_0),$$

where (x_0, z_0) is a reference point. Thus, the velocity distribution is written in the form

$$v(x,z) = v_0(x,z) + \lambda_1 + \lambda_2(z - z_0) + \lambda_3(x - x_0), \tag{12}$$

where v_0 is a background velocity. An imaged depth depends on only the velocity above it, except for turning rays. Therefore, use of a recursive algorithm (layer stripping) is possible to determine velocity in an individual block. We start from the block nearest surface. For example, we choose the top left block in Figure 1. In each block, iteration is used to calculate velocity parameters. Given an initial guess for λ_i's, prestack depth migration is implemented to obtain imaged depths and $g_i(x,h)$ in equation (10) for common image gathers that will give a correction of the parameters. Then by using the updated parameters as an initial guess, we correct the velocity again until convergence is achieved. After velocity analysis in one block, we migrate data with the corrected velocity, and pick the velocity interface from the

imaged structures. When velocity and velocity interface determining is finished in one block, we will repeat the same procedure to the next block that is located directly below the finished block.

The layer-stripping procedure for velocity analysis can be stated as follows:

- begin with the first block
  1. estimate velocity parameters iteratively
     (a) migrate with an initial guess of velocity;
     (b) sort the migrated data into common image gathers;
     (c) measure imaged depths and evaluate the derivative function;
     (d) update velocity by using the perturbation formula;
  2. image velocity interface by using corrected velocity
- repeat step 1 and 2 for next block (recursion)

When velocity and velocity gradients are estimated simultaneously in a given block, the iteration tends to be unstable. To overcome this difficulty, it is preferable to estimate velocity first. This estimation will yield an average velocity and give a better initial guess for the velocity gradients in this block.

COMPUTER IMPLEMENTATION

The Marmousi data set is generated by using a two-dimensional acoustic finite-difference modeling program. The model contains many reflectors, steep dips, and strong velocity variations in both lateral and vertical directions (with a minimum velocity of 1500 m/s and a maximum velocity of 5500 m/s), shown in Figure 2. The data set consists of 240 shots with 96 traces per shot. The initial offset is 200 m; both the shot and receiver spacings are 25 m. The first shot is at lateral position 3000 m. Nineteen common-offset data gathers with offsets ranging from 200 m to 2000 m are used for velocity analysis. The selected offsets range from 200 m to 2000 m with spacing 100 m. The minimum-offset gather is shown in Figure 3.

During the velocity analysis process, we assume that the velocity field is a macro model and that the velocity distribution is a linear function in each block. Velocity analysis results surely depend the choice of migration algorithm used. There are two commonly used approaches to calculate traveltimes in Kirchhoff migration: finite differencing and ray tracing. Compared to ray tracing, the finite differencing approach is easier to code and more efficient to implement, but fails to correctly image complicated structures when multiple arrivals exist (Geoltrain and Brac, 1993).

A finite differencing traveltime solver is initially used in the migration implementation for velocity analysis in the area where the first arrivals carry the major energy. The estimated velocity model is shown in Figure 4. In the central bottom parts,

a paraxial ray tracing algorithm is used to implement Kirchhoff migration. In this approach, the traveltime corresponding to the major energy is chosen when multiple arrivals exist.

Using the Kirchhoff migration algorithm by paraxial ray tracing, velocity analysis is done through the central bottom parts of the Marmousi model. The updated velocity model, shown in Figure 5, consists of 19 blocks. In each block, the velocity distribution is a constant or linear function of the depth. Comparison of the estimated velocity model with the true one at three lateral locations is shown Figure 6. One can see that the estimated velocity matches the true model well except for thin layers. In fact, from sensitivity analysis (Liu, 1995), velocities in these thin layers cannot be determined well. The stacked migration section using the velocity model in Figure 5 is shown in Figure 7. Compared to the migration result using the true velocity model, shown in Figure 8, Figure 7 gives an acceptable structural image even in the central bottom parts, which indicates the capability of this migration velocity analysis approach for handling complex structures. The subsurfaces are well imaged except for some detailed features in the central bottom parts. Some blurry image in the central bottom parts may be caused by missing high-velocity zones. Figure 2 shows that the true velocity model contains several small high-velocity zones in the central parts. These high-velocity zones do not appear in Figure 5 because of the limitations of velocity analysis and the resolution of migration imaging.

Selected common image gathers from migrated data using the estimated model are shown in Figures 9, 10 and 11, representing the left, central and right parts of the model respectively. The alignment of reflections in Figures 9, 11 and the upper part of Figure 10 indicates the correctness of the estimated velocity in these areas. The bottom part of Figure 10 shows incoherent signals that limit the accuracy of velocity estimation in this particular area. Notice that, at the same common-image gathers (see Figure 12), migrated data using the true velocity also contain obvious incoherency in residual moveouts, although the stacked section shows a good image. This example demonstrates that for an extremely complex structure it is difficult to identify the correct velocity model based on the criterion of kinematic coherence.

CONCLUSION

Imaging complex structures (such as the Marmousi data) requires effective prestack depth migration algorithms as well as advanced velocity analysis techniques. The perturbation method in this paper provides a useful tool for updating a velocity model by matching a criterion based on kinematic coherence of the prestack migrated images, which is one of the key elements in velocity model determination (Versteeg, 1994). In order to obtain a more satisfactory velocity analysis result for a complicated model, as Versteeg concluded, one also needs related geologic information as constraints.

REFERENCES

Beydoun, W. B., and Keho, T. H., 1987, The paraxial method: Geophysics, **52**, 1639-1653.

Bleistein, N., Cohen, J., and Hagin, F., 1987, Two and one-half dimensional Born inversion with an arbitrary reference: Geophysics, **52**, 26-36.

Geoltrain, S., and Brac, J., 1993, Can we image complex structures with first-arrival traveltime migration: Geophysics, **58**, 564-575.

Liu, Z., 1995, Migration velocity analysis: Ph. D. thesis, Colorado School of Mines. Center for Wave Phenomena Research Report number CWP-168.

Liu, Z., and Bleistein, N., 1994, Velocity analysis by perturbation: 1994 SEG expanded abstracts, p. 1191.

Versteeg, R., 1994, The Marmousi experience: velocity model determination on a synthetic complex data set: The Leading EDGE, **13**, 927-936.

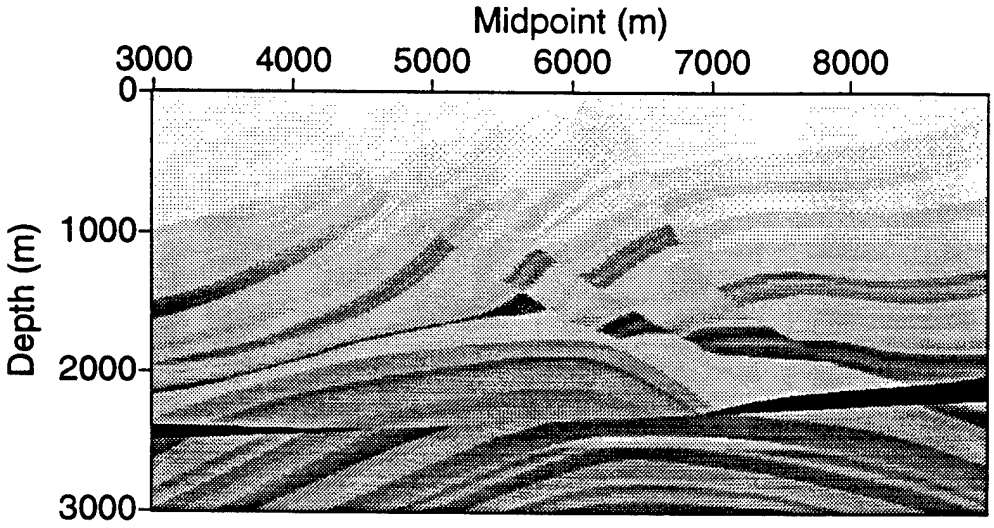

FIG. 2. The Marmousi velocity model. The darker shading denotes higher velocity.

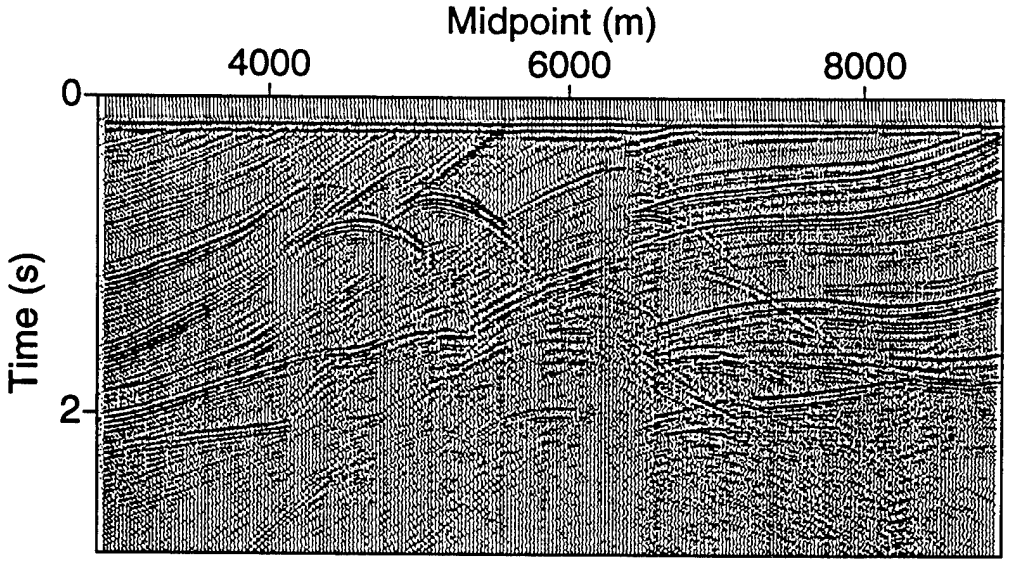

FIG. 3. The minimum-offset Marmousi data. The offset is 200 meters.

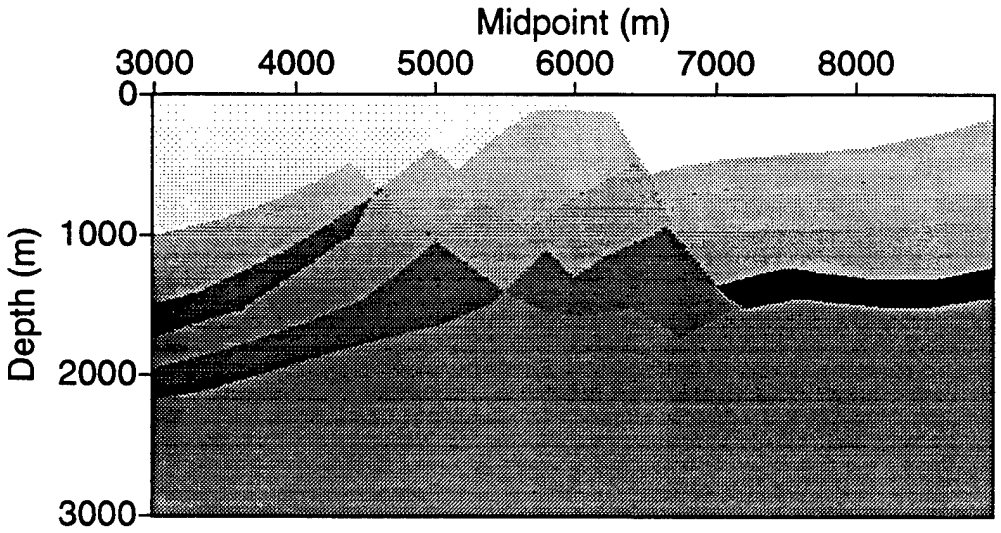

FIG. 4. The estimated velocity model using the first-arrival operater.

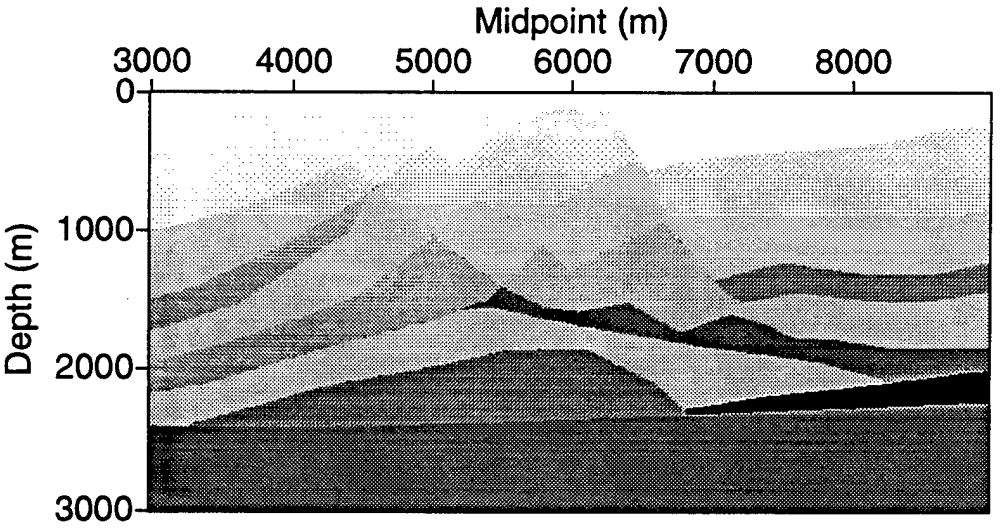

FIG. 5. The updated velocity model using the paraxial ray tracer.

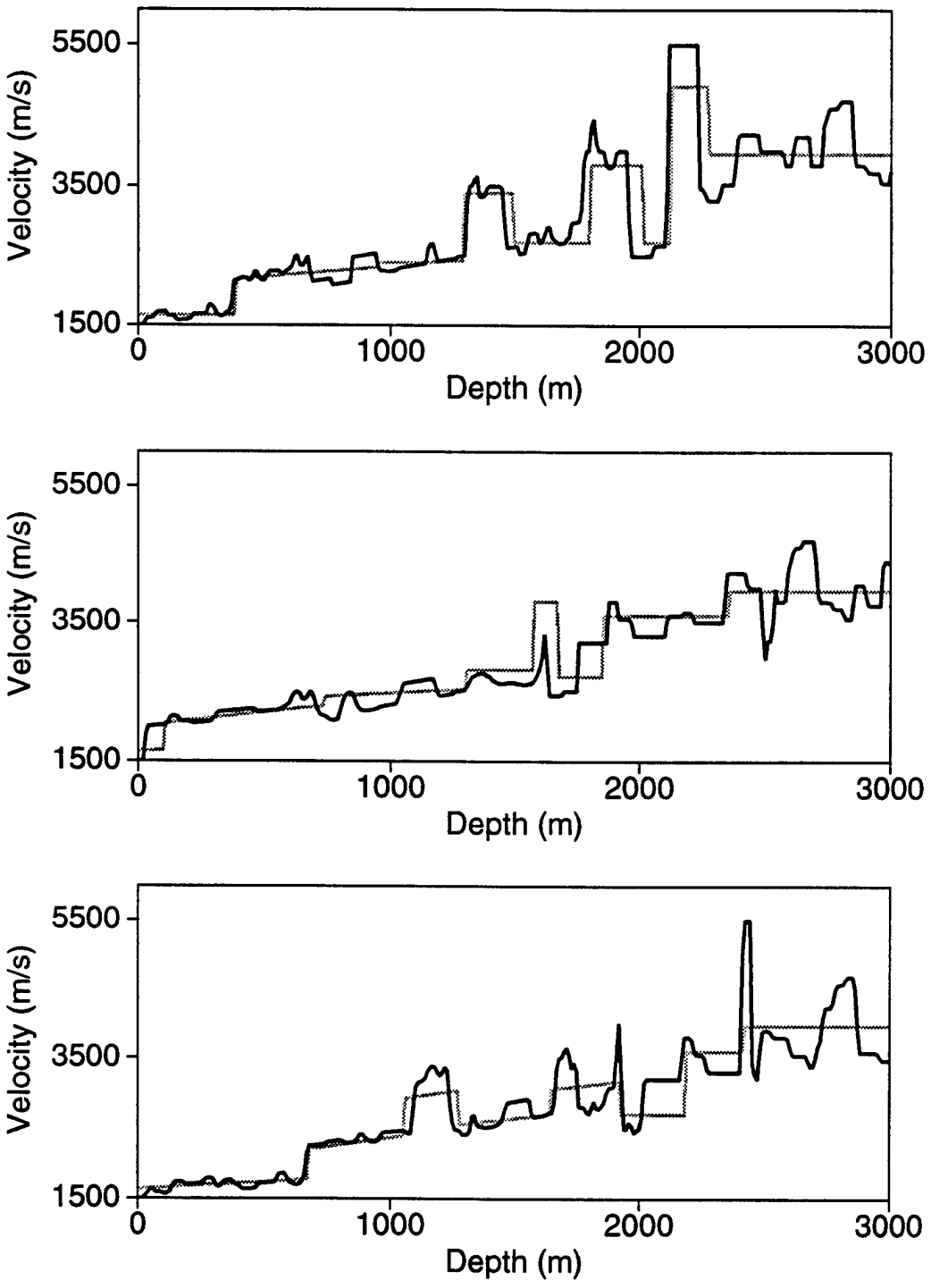

FIG. 6. Comparison of the true velocity model with the estimated one. The dark curve denotes the true velocity and the gray denotes the estimated velocity. The top figure is at location x=8 km; the middle, at location x=6 km; the bottom, at location x=4 km.

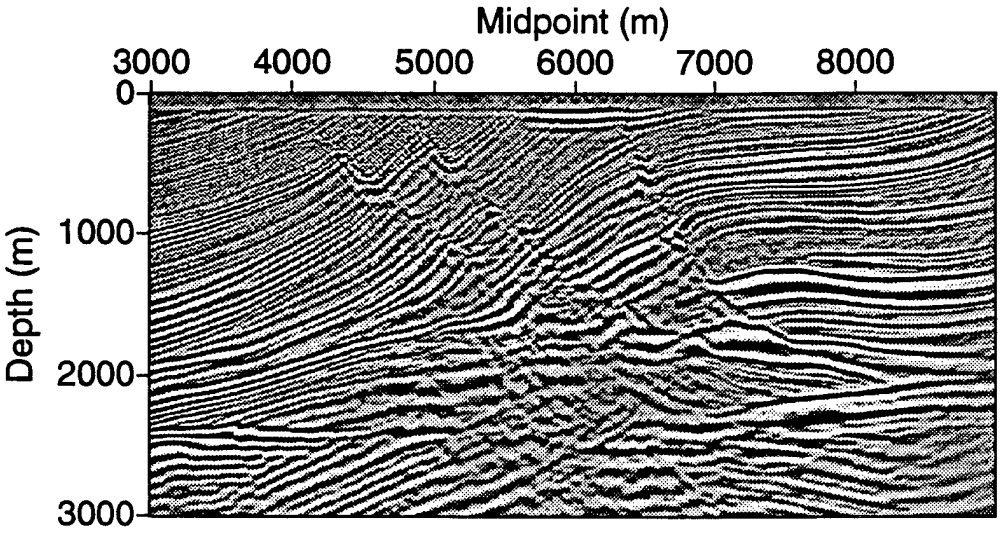

FIG. 7. 19-offset stacked migration output for the Marmousi data. The input velocity is one in Figure 6.

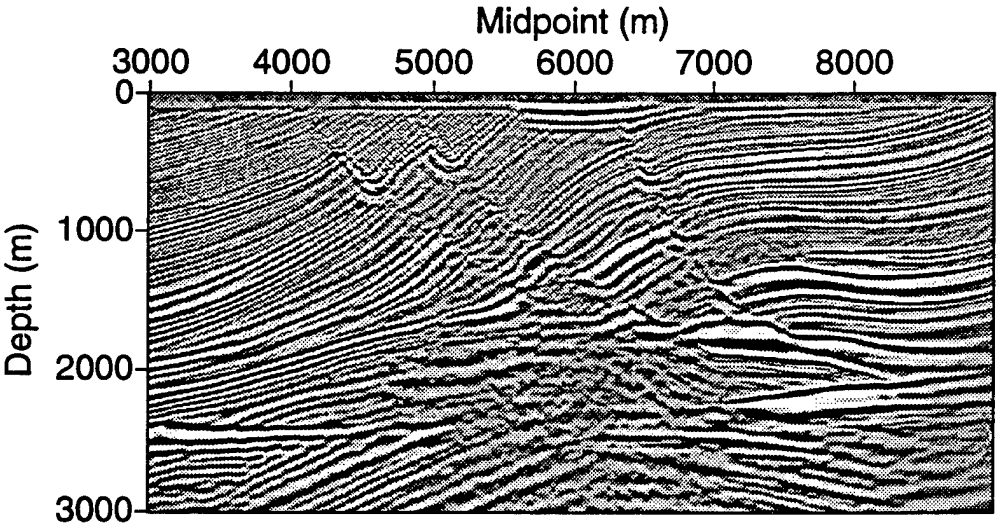

FIG. 8. 19-offset stacked migration output for the Marmousi data. The true velocity is used.

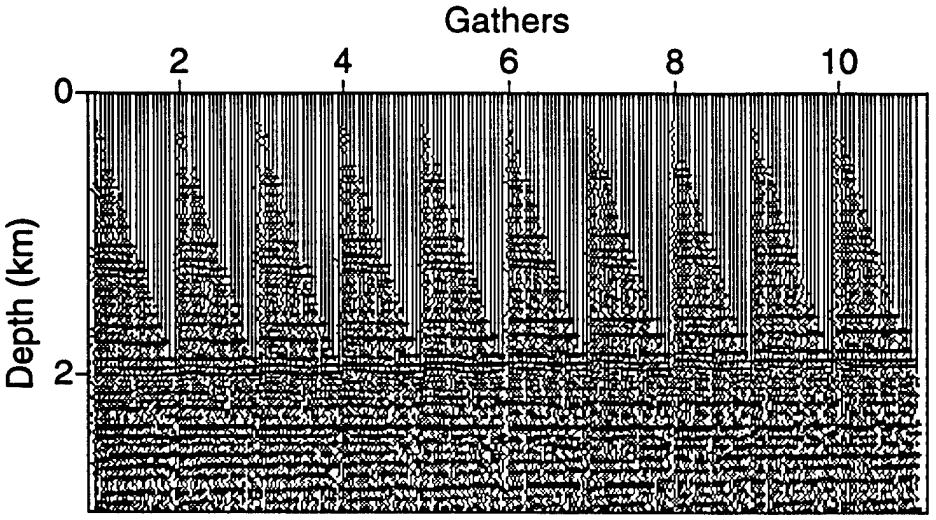

FIG. 9. Ten common image gathers. 19 offsets in each CIG. The image location ranges from 4 km to 4.25 km.

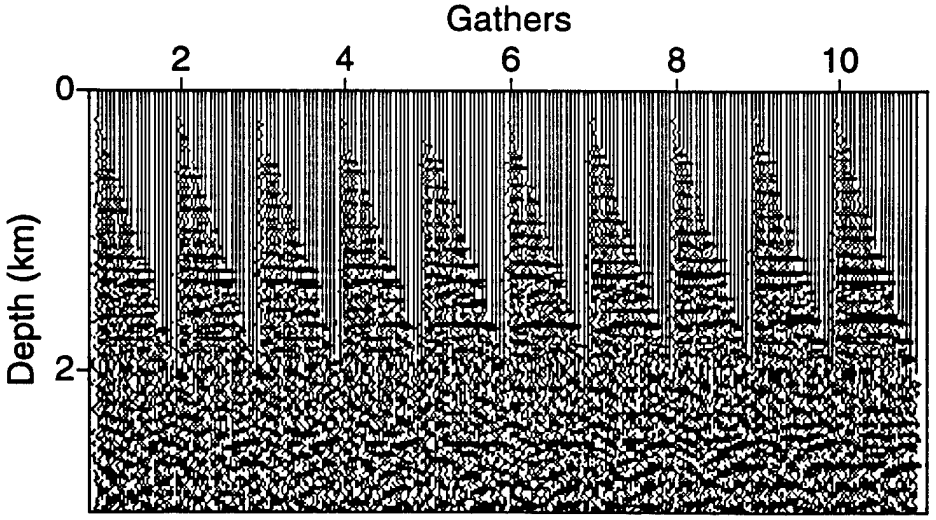

FIG. 10. Ten common image gathers. 19 offsets in each CIG. The image location ranges from 6 km to 6.25 km.

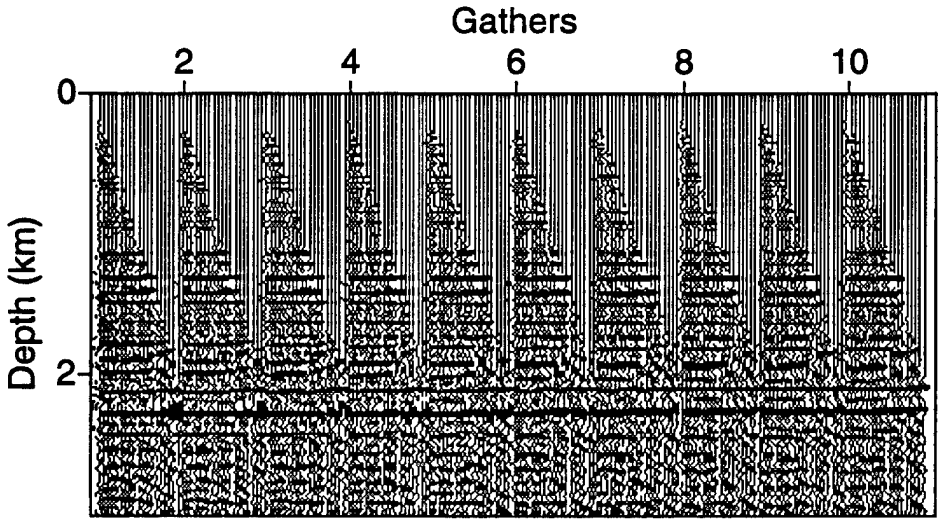

FIG. 11. Ten common image gathers. 19 offsets in each CIG. The image location ranges from 8 km to 8.25 km.

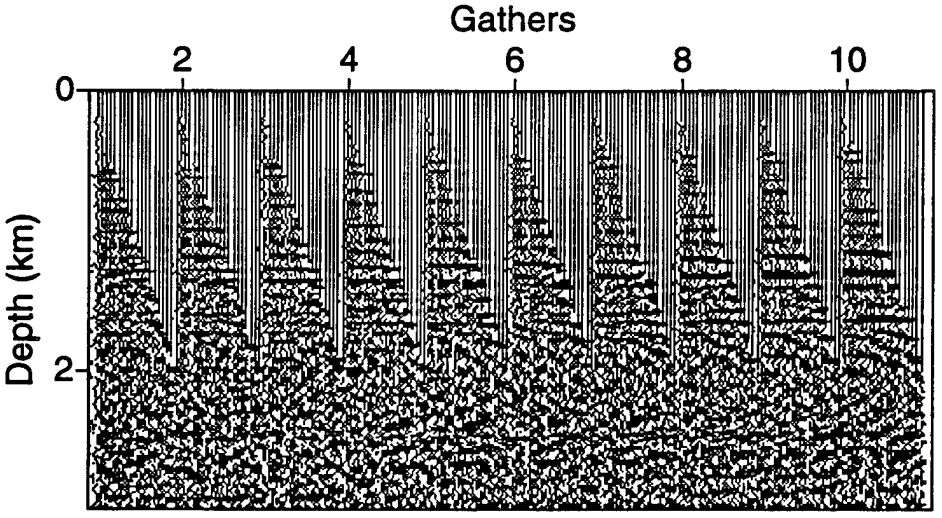

FIG. 12. Ten common image gathers from migrated data using the true velocity. The image location ranges from 6 km to 6.25 km.